PRIMERJAVA URADNEGA KVAZIGEOIDNEGA MODELA SRBIJE Z NEKATERIMI GLOBALNIMI GEOPOTENCIALNIMI MODELI

VALIDATION AND COMPARISON OF SEVERAL GLOBAL GEOPOTENTIAL MODELS WITH AN OFFICIAL QUASIGEOID SOLUTION OF SERBIA

Marko D. Stanković, Oleg R. Odalović, Miloš D. Marković

UDK: 528.21(497.11)
Klasifikacija prispevka po COBISS.SI: 1.04
Prispelo: 28. 2. 2022
Sprejeto: 20. 7. 2022

DOI: 10.15292/geodetski-vestnik.2022.03.432-448
PROFESSIONAL ARTICLE
Received: 28. 2. 2022
Accepted: 20. 7. 2022

IZVLEČEK

V raziskavi smo primerjali uradni kvazigeoidni model Srbije (SQM2011) s tremi lokalnimi kvazigeoidnimi ploskvami, ki smo jih izračunali na osnovi treh globalnih geopotencialnih modelov (GGM): GOCO05c, SGG-UGM-2 in XGM2019e. Izračunane anomalije višin smo primerjali na 1001 točki mreže preciznega nivelmana, na katerih so nam znane nadmorske in elipsoidne višine. Na osnovi izračunanih razlik na teh točkah smo določili transformacijski model, ki je omogočal izračun končnih vrednosti anomalij višin na 143.207 točkah gridne mreže v ločljivosti 0,5' × 0,5' na območju celotnega ozemlja Srbije. Analiza je pokazala najboljše ujemanje za globalni geopotencialni model SGG-UGM-2, pri čemer so statistični kazalci preostalih razlik: srednja vrednost 0,01 m, standardni odklon 0,06 m in razpon razlik 0,67 m.

KLJUČNE BESEDE

globalni geopotencialni model, anomalije višin, kvazigeoid, gravitacija, GNSS/dh

ABSTRACT

This study aims to analyze the quality of several local reference quasigeoid surfaces obtained from several Global Geopotential Models (GGM) relative to the official quasigeoid solution of Serbia (SQM2011) and GNSS/dh observations for the territory of Serbia. Therefore, validation and comparison of the derived surfaces from the three GGM's were made based on comparisons of height anomaly derived from GGM's, SQM2011, and the GNSS/dh observations at the points of the high-precision leveling network. The selected publicly available GGM's in this study are GOCO05c, SGG-UGM-2, and XGM2019e. Primarily, at 1001 points of the high-precision leveling network, the differences between GGM and GNSS/dh height anomaly were calculated. The final translation parameters were calculated in the iteration procedure, which was then used to calculate the final values of the estimated height anomaly for all GGM's at 143207 points of the regular grid of spatial resolution 0.5' × 0.5' on the entire territory of Serbia. From the estimated height anomaly, three GGM-derived surfaces were modeled relative to the SQM2011. According to the results of the calculations, SGG-UGM-2 provides the best approximation of the quasi-geoid SQM2011, where the remaining differences have a mean value of 0.01 m, a standard deviation of 0.06 m, and a span of 0.67 m.

KEY WORDS

Global Geopotential Model, height anomalies, quasigeoid, gravity, GNSS/dh

INTRODUCTION

This research aims to validate and compare GGM-derived local reference surfaces from three selected global geopotential models or abbreviated GGM's (GOCO05c, SGG-UGM-2, and XGM2019e) with the SQM2011 and available data from GNSS/dh (GNSS-levelling) observations. The aim is to determine the achieved real quality of these surfaces, which directly depends on the quality of the used data available for the territory of Serbia and used GGM's. After the conclusions, it is necessary to give a proposal and define the direction of development of a local reference surface model for the part or the entire territory of Serbia for the needs of geodesy, geophysical research, engineering projects, topographic surveying, height determination with GNSS methods, vertical datum definition and unification. Over time, GGM's have significantly advanced in terms of the degree and order, which is primarily the result of defining GGM's based on combined data sets obtained from a variety of sources such as altimetric observations over the seas and oceans, satellite observations, and tracking of satellite trajectories (such as GRACE, GOCE, and LAGEOS), terrestrial observations by various methods on land, seas, oceans, and from the air, and topography data. Combining these data sets from diverse sources in defining a single GGM provides higher quality, better territorial coverage, more homogeneous GGM data accuracy for most of the global territory, and a more refined model surface due to the higher degree and order of the model.

In defining SQM2011 (Ågren, J. et al., 2012) used the satellite-only model GOCO02s, which is of a much lesser degree and order compared to today's GGM's, and since it is a satellite-only model, the long-wavelength characteristic is limited due to the satellite-only data sources in GGM. On the other hand, data obtained from the GNSS/dh observations at the points of high precision leveling network on the territory of Serbia are accompanied by many problems because the data were obtained using different methods and instruments in different periods. There is also the problem of old available data and stability of some points. All this means that these data are of inhomogeneous and questionable quality. These mentioned problems are why a certain number of points were rejected or not used in the direct determination of SQM2011. These facts are more than enough to raise whether it is necessary to define a new height reference surface based on more modern and advanced GGM's and new terrestrial data, but that is a question for some future scientific endeavors. The validation of GGM-derived local reference surfaces was done using three modern GGM's relative to SQM2011 and combined with GNSS/dh observations at the high precision leveling network points for which there is some security. Therefore, it is necessary to have reliable information that the points are stable and that the observations were made simultaneously, with the same accuracy and method. Then it can be claimed with some certainty that the results are of the same accuracy. Future local reference surfaces must be defined in the most modern ways of modeling geoids and quasigeoids based on terrestrial gravity and topographic data in combination with the most modern combined GGM. Significant improvements in modeling local or national models of geoids and quasigeoids depend on improved terrestrial data sets and the GGM's based on modern satellite missions (GOCE and GRACE). Based on results of GNSS/dh observations, there are estimates of the accuracy of modern European gravimetric quasigeoids on a national (local) basis from 1 cm to 2 cm and on the continental level from 2 cm to 4 cm, where the available input data must be of high quality and resolution in the territory of interest.

2 SERBIAN QUASIGEOID MODEL 2011 – SQM2011

Since the reference surfaces are determined for the territory of Serbia, it is necessary in this chapter to briefly describe the used data sources and calculation procedure of SQM2011. For more detailed information, the reader is referred to the report of Ågren, J. et al., 2012. The report is not publicly available, but it can be obtained on request from the Republic Geodetic Authority in Serbia. In quasigeoid computing, there is a wide variety of approaches. When quasigeoid is derived from gravity data, a digital terrain model, and a global geopotential model, the remove-compute-restore (RCR) methodology is utilized most frequently. The goal is, after determining the gravimetric model, it should be adapted to the local (national) reference system using GNSS/dh height anomaly, which is defined as the differences between GNSS-determined heights above the ellipsoid and leveled normal heights at the same points on the physical surface of the Earth. Statistics properties of SQM2011-derived height anomaly $\zeta^{SQM\,2011}$ at the points of the high-precision leveling network are given in Table 1, and surface data is shown in Figure 1.

Table 1: Characteristic values of SQM2011-derived height anomaly at 1001 points (unit: meter).

ζ	$\zeta_{\min}$	$\zeta_{\max}$	$\zeta_{average}$	ζ_{range}	$\sigma_{\zeta\,(STDEV)}$
$\zeta^{SQM\,2011}$	42.31	46.38	44.62	4.07	0.85

SQM2011 is based on the following data sets: gravity data on the territory of Serbia, normal heights of the stations, gravity data in the neighboring countries, digital terrain models (DTM's), GGM's (EGM2008, at the time, the most suitable model and satellite-only model GOCO02s), GNSS/dh geoid heights and heights above the ellipsoid (ETRS 89) (Ågren, J. et al., 2012). The data used in calculating the gravimetric model are the existing gravimetric data on the territory of Serbia. The method used is Least Squares Modification of Stokes' formula with Additive corrections (LSMSA), i.e. (KTH method) of Sjöberg, L. E. (1991, 2003a, 2003b) and Sjöberg, L. E. et al., 2000, together with the latest satellite-only global geopotential model GOCO02s. In border areas, EGM2008-derived gravity anomalies on the area-means grid of spatial resolution 5' × 5' were used to obtain information on high-frequency gravity anomalies for the border areas approximately from 200 km to 300 km in the territory of those neighboring countries where no data of gravity observations were available.

After computing the gravimetric model, a comparison and fitting with GNSS/dh observations at FR – (points of national leveling network) and SREF – (Serbian passive GNSS network) points was made (Veljković, Z. et al., 2011 and Vušović, N. et al., 2013). Comparison and fitting were made by a four-parameter transformation model based on the following equation,

$$h_i - H_i^o - N_i = \cos(\varphi_i)\cos(\lambda_i)b_0 + \cos(\varphi_i)\sin(\lambda_i)b_1 + \sin(\varphi_i)b_2 - b_3\,, \tag{1}$$

where H_i^o is the benchmark orthometric height, h_i is the ellipsoidal (geometric) height derived from GPS measurements, N_i is the gravimetric geoid height (undulation) predicted at GPS/benchmarks, b_0, b_1, b_2, b_3 are the translation parameters of the model, and φ_i, λ_i are the benchmarks' coordinates (latitudes and longitudes).

After all, a smooth residual surface based on least square collocation was created to transform ellipsoidal heights to normal height (Ågren, J. et al., 2012).

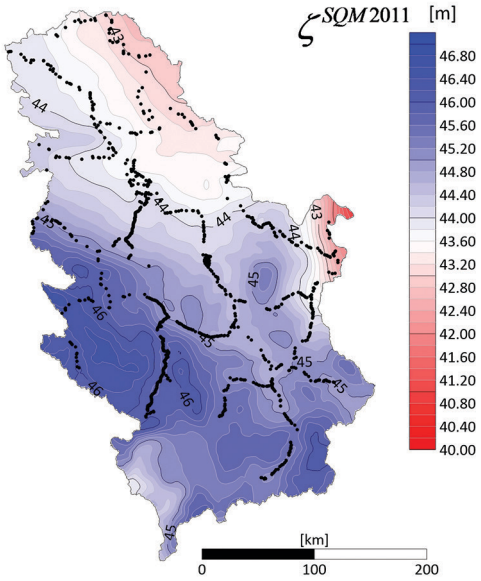

Figure 1: The contour plot (map) of SQM2011 with points of GNSS/dh high precision leveling network (*n*=1001).

3 GLOBAL GEOPOTENTIAL MODELS GOCO05C, SGG-UGM-2, AND XGM2019E – PUBLICLY AVAILABLE DATA

Over the last 50 years, many researchers and scientific organizations have created GGMs. Their work has been published online and is available for research and work to the scientific and technical public. Five internet sites publish finished models with data, explanations, and other GGM-related material. The International Association of Geodesy coordinates these services (IAG). International Centre for Global Earth Models (ICGEM); Bureau Gravimetrique International (BGI); International Service for the Geoid (ISG); EOST's International Geodynamics and Earth Tide Service (IGETS); ESRI's International Digital Elevation Model Service (IDEMS). When drafting this research, ICGEM had 177 global geopotential models.

3.1 Mathematical background and application of GGM

The mathematical function that approximates the Earth's gravity field in three-dimensional space outside the body of the Earth is called the global geopotential model, the gravity field model, or the global model (Barthelmes, 2014). As a function of spherical harmonics, the gravity potential of the Earth's gravity can be represented as:

$$W(r,\theta,\lambda)=\frac{GM}{a}\sum_{n=0}^{\infty}\left(\frac{a}{r}\right)^{n+1}\sum_{m=0}^{n}\left[\overline{C}_{nm}\cos(m\lambda)+\overline{S}_{nm}\sin(m\lambda)\right]\overline{P}_{nm}(t)+\frac{1}{2}\omega^2 r^2\sin^2(\theta), \qquad (2)$$

and normal potential:

$$U(r,\theta,\lambda)=\frac{GM}{a}\sum_{n=0(2)}^{\infty(8)}\left(\frac{a}{r}\right)^{n+1}\overline{C}_{nm}^{U}\overline{P}_{nm}(t)+\frac{1}{2}\omega^2 r^2\sin^2(\theta), \tag{3}$$

where are: $\overline{C}_{nm}$ and $\overline{S}_{nm}$ are unknown coefficients, fundamental physical constants (G, M, ω) that can be considered already determined for applying the expression (2), and coordinates of points (r, θ, λ) that are relatively easy to determine today (Odalović, O., 2010 and Odalović, O. et al., 2012, 2018a, 2018b, 2020). To apply the equations (2) and (3), coefficients must be determined to a specific degree n and order m, using satellite-only data sets or a combination of satellite-only and terrestrial data sets for most of the world's territory, and a more refined model surface due to the higher degree and order of the model. Only satellite trajectory observation data can be used to estimate coefficients for satellite data groups. The relationship between spherical harmonic expansion coefficients and changes in Kepler satellite trajectory parameters (Heiskanen & Moritz, 1967) is used to study the Earth's gravity field. Gravity field satellite missions include CHAMP (Reigber et al., 2003), GRACE (Adam, 2002), and GOCE (Gravity Field and Steady-State Ocean Circulation Explorer) (Rebhan et al., 2000). From satellite-only data sets, low-grade solutions can be defined. Satellite solutions are combined with terrestrial measurements, gravity anomalies, discrete height anomalies, or geoid undulations to create global geopotential models (Pavlis et al., 2012). All the essential data from several worldwide geopotential models are online as text files, and their archives are classified into Static Models and Temporal Models. For the purposes of this research, 25 GGM's were tested, among which three GGM's were singled out, which were found to best approximate the discrete values of height anomalies for the territory of Serbia. This paper employed three global models: GOCO05c (Fecher et al., 2015, 2017, 2020), XGM2019e_2159 (Zingerle, P. et al., 2020), and SGG-UGM-2 (Liang, W. et al., 2020). These worldwide models are summarized below.

4 THE GNSS/DH OBSERVATIONS

On the points of the GNSS/dh high-precision leveling network on the territory of Serbia, GNSS/dh height anomalies were calculated as differences between the heights determined by GNSS observations relative to the GRS80 ellipsoid in ETRF 2000 and leveled normal heights in the leveling network of high precision (Nivelman visoke tačnosti 2– NVT2) at the same observation points. Many network points are located in valleys and lowlands, with the rest at higher altitudes and near mountains. To determine SQM2011, the model's authors used 1130 points (Ågren, J. et al., 2012). The ellipsoidal heights were obtained using several GNSS approaches. The static GNSS approach was employed in the limited number of observations to calculate SREF stations and NVT2 fundamental benchmarks. However, a significant number of GNSS/dh observations were made via Network RTK. Disadvantages that need to be emphasized are: the normal heights of the NVT2 network points are determined differently, which is the reason for their inhomogeneous quality, there is no small uncertainty in the stability of the benchmarks, and the standard errors of the benchmark should also reflect the possibility of the influence of systematic errors of the height system at longer distances, and due to the impact of unmodelled systematic errors and time correlations, the actual standard errors are not corresponding to the formal standard errors (Ågren, J. et al., 2012). In validating GGM-derived local reference surfaces in this research, 1001 points

of the high-precision leveling network were included, on which GNSS/dh observations were performed. The reason for using 1001 points instead of 1130 is because only those points were available from the Republic Geodetic Authority, and all the data for available points we received show a high agreement with the SQM2011 solution and there are no outliers. The remaining 129 points were not available to us. Table 2 contains statistical properties from height anomaly from 1001 points.

Table 2: Statistical properties of GNSS-derived height anomaly at 1001 points (unit: meter).

ζ	$\zeta_{\min}$	$\zeta_{\max}$	$\zeta_{average}$	ζ_{range}	$\sigma_{\zeta(STDEV)}$
$\zeta^{GNSS/dh}$	42.33	46.41	44.64	4.08	0.85

Figure 2 presents the validation and comparison of GGM-derived local reference surfaces with SQM2011 and GNSS/dh observations as an algorithm for more profound insight into the calculations processes and understanding of the research's aim. Calculations are presented as tables and graphical maps showing height anomalies before and after two iterations and estimated differences in 1001 points of the high-precision leveling grid. The results are shown in tables and on a contour plots (maps) of estimated height anomaly from three GGM's and SQM2011 calculated from the gridded residuals on 1001 points at 143207 points on a regular grid (contour map).

5 NUMERICAL RESEARCH

5.1 Calculation procedure on GNSS/dh high-precision leveling network

The original calculations refer to a high-precision leveling network of 1001 points (P_i, $i \in (1, 1001)$). Coordinates latitudes φ_i, longitudes λ_i, normal heights H_i, GNSS/dh-derived height anomaly $\zeta_i^{GNSS/dh}$, and SQM2011-derived height anomaly $\zeta_i^{SOM\,2011}$ are available for all network points. Also, GGM height anomalies are derived at the same network points (Table 3). The derivation procedure of GGM height anomaly is based on the three selected GGM's.

Table 3: Characteristic values of ζ^{GGM} at 1001 points (unit: meter).

ζ^{GGM}	$\zeta_{\min}$	$\zeta_{\max}$	$\zeta_{average}$	ζ_{range}	$\sigma_{\zeta(STDEV)}$
$\zeta^{GOCO05c}$	42.29	46.16	44.59	3.87	0.88
$\zeta^{SGG-UGM-2}$	42.28	46.25	44.52	3.97	0.83
$\zeta^{XGM\,2019e}$	42.25	46.17	44.51	3.92	0.82

At the points of a high-precision leveling network (GNSS/dh grid), the differences $t_i^{GOCO05c}$ $t_i^{SGG-UGM-2}$ and $t_i^{XGM\,2019e}$ (where is $i \in (1, 1001)$) between the values of the height anomaly of the GGM's and GNSS/dh were calculated (for each model individually):

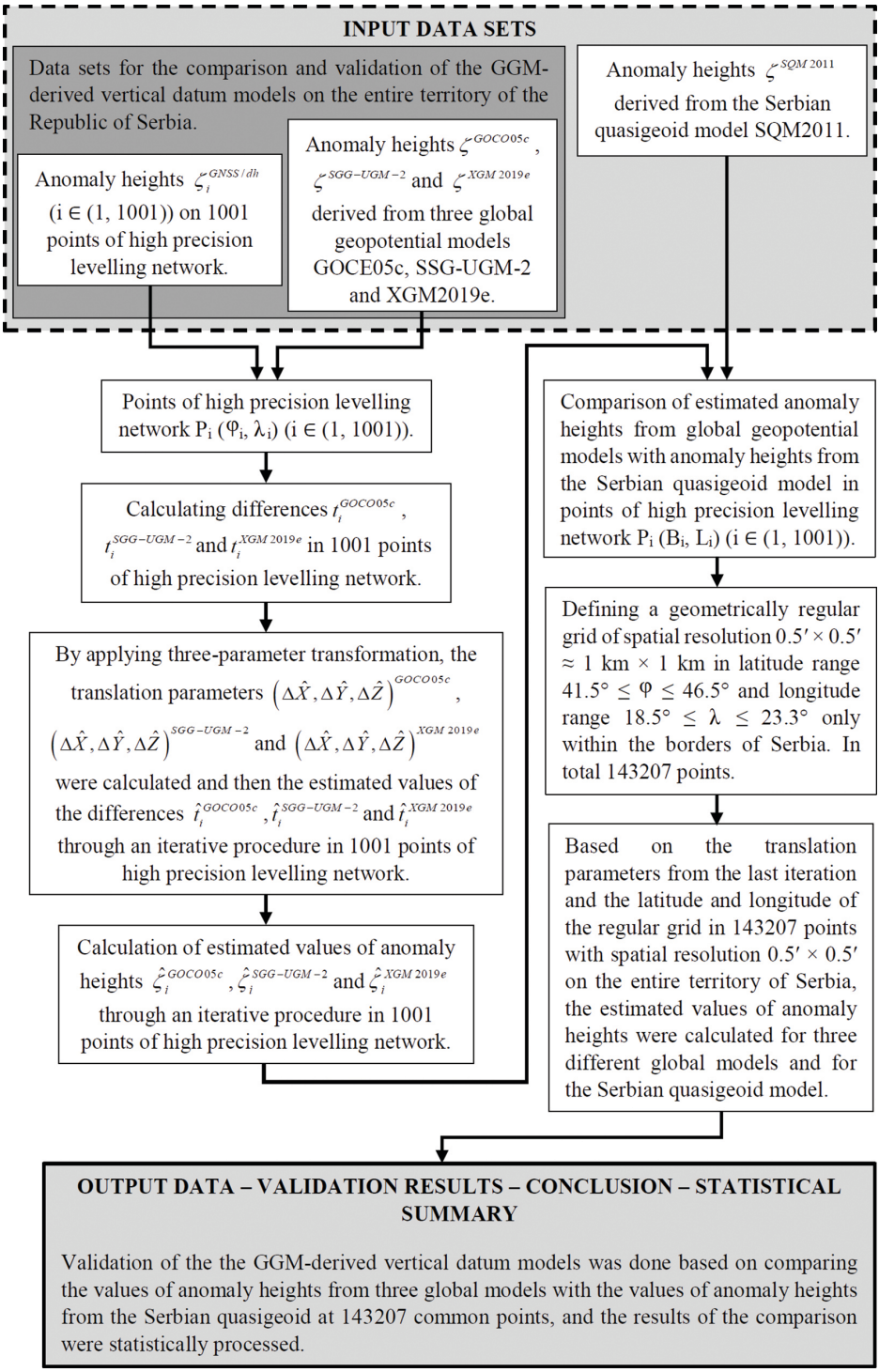

Figure 2: Structure of SQM2011 validation and comparison algorithm.

$$t_i^{GGM} = \zeta_i^{GGM} - \zeta_i^{GNSS/dh}, \tag{4}$$

where t_i^{GGM} are the differences between height anomaly from GOCO05c, SGG-UGM-2, and XGM2019e models and GNSS/dh (Figure 3). Height anomaly ζ_i^{GGM} can represent elements of three data sets whose values are GGM-derived from GOCO05c, SGG-UGM-2, and XGM2019e. The obtained values were statistically processed, and for each was obtained: average value , $t_{average}^{GGM}$ minimum value t_{min}^{GGM} , maximum value t_{max}^{GGM} , range t_{range}^{GGM} , and standard deviation σ_t^{GGM} (Table 4).

Table 4: Statistics of t^{GGM} (unit: meter).

t^{GGM}	$t_{\min}$	$t_{\max}$	$t_{average}$	t_{range}	$\sigma_{t(STDEV)}$
$t^{GOCO05c}$	-0.33	0.21	-0.05	0.54	0.10
$t^{SGG-UGM-2}$	-0.49	0.09	-0.12	0.58	0.07
$t^{XGM2019e}$	-0.42	0.09	-0.13	0.51	0.08

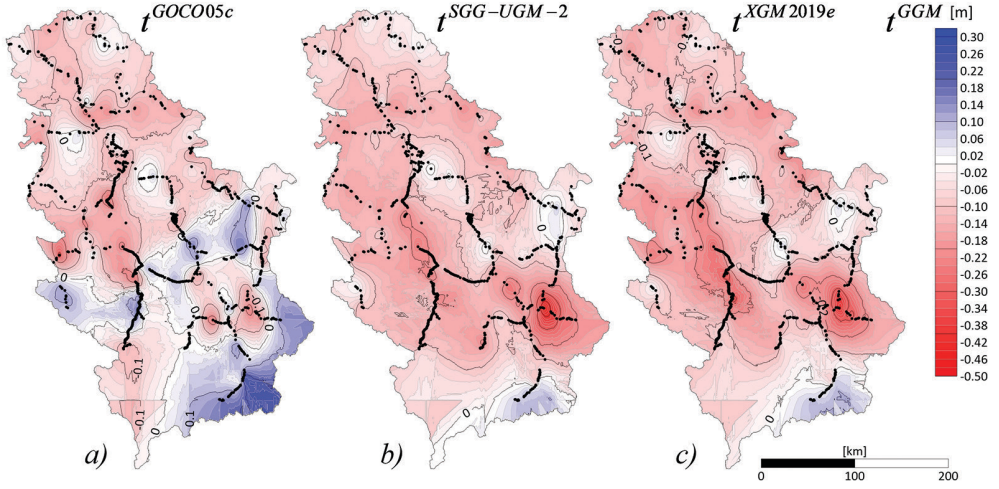

Figure 3: Contour map (plot) of t^{GGM} for a) GOCO05c, b) SGG-UGM-2 and c) XGM2019e (n=1001).

Starting from three-parameter transformation (equation (5)):

$$\hat{t}_i = \cos(\varphi_i)\cos(\lambda_i)\Delta\hat{X} + \cos(\varphi_i)\sin(\lambda_i)\Delta\hat{Y} + \sin(\varphi_i)\Delta\hat{Z}, \tag{5}$$

and based on the coefficients from the equation (5) and latitudes φ_i and longitudes λ_i of the points P_i ($i \in (1, 1001)$), a design matrix $\mathbf{A}_{n\times 3}$ and weight matrix $\mathbf{P}_{n\times n}$ were formed according to the following principle:

$$\mathbf{A}_{n\times 3}=\begin{bmatrix}\cos(\varphi_1)\cos(\lambda_1) & \cos(\varphi_1)\sin(\lambda_1) & \sin(\varphi_1)\\ \vdots & \vdots & \vdots\\ \cos(\varphi_i)\cos(\lambda_i) & \cos(\varphi_i)\sin(\lambda_i) & \sin(\varphi_i)\\ \vdots & \vdots & \vdots\\ \cos(\varphi_n)\cos(\lambda_n) & \cos(\varphi_n)\sin(\lambda_n) & \sin(\varphi_n)\end{bmatrix}_{n\times 3} \quad \text{and} \quad \mathbf{P}_{n\times n}=\begin{bmatrix}1 & 0 & 0 & 0\\ 0 & 1 & 0 & 0\\ \vdots & \vdots & \ddots & \vdots\\ 0 & 0 & \cdots & 1\end{bmatrix}_{n\times n} \tag{6}$$

The vector of free terms $\mathbf{f}_{n\times 1}$ is given by subtracting the difference t from the mean $t_{average}^{GGM}$:

$$\mathbf{f}_{n\times 1}=\begin{bmatrix}t_{average}^{GGM}-t_1^{GGM}\\ \vdots\\ t_{average}^{GGM}-t_i^{GGM}\\ \vdots\\ t_{average}^{GGM}-t_n^{GGM}\end{bmatrix}_{n\times 1}, \tag{7}$$

where n=1001. Design matrix $\mathbf{N}_{3\times 3}$, cofactor matrix $\mathbf{Q}_{\mathbf{x}3\times 3,}$ and vector $\mathbf{n}_{3\times 1}$ were obtained as:

$$\mathbf{N}_{3\times 3}=\mathbf{A}_{3\times n}^{\mathrm{T}}\mathbf{P}_{n\times n}\mathbf{A}_{n\times 3}=\mathbf{A}_{3\times n}^{\mathrm{T}}\mathbf{A}_{n\times 3} \quad , \quad \mathbf{Q}_{\mathbf{x}3\times 3}=\mathbf{N}_{3\times 3}^{-1} \quad \text{and} \quad \mathbf{n}_{3\times 1}=\mathbf{A}_{3\times n}^{T}\mathbf{P}_{n\times n}\mathbf{f}_{n\times 1}=\mathbf{A}_{3\times n}^{T}\mathbf{f}_{n\times 1}\ . \tag{8}$$

Finally, the vector $\mathbf{f}_{n\times 1}$of the estimated parameters $\hat{\mathbf{X}}_{3\times 1}$ is calculated as:

$$\hat{\mathbf{x}}_{3\times 1}=-\mathbf{n}_{3\times 1}\mathbf{Q}_{\mathbf{x}3\times 3}=\begin{bmatrix}\Delta\hat{X}\\ \Delta\hat{Y}\\ \Delta\hat{Z}\end{bmatrix}. \tag{9}$$

In order to simplify the method as much as possible, we used a three-parameter transformation, that is, only translations along the X, Y, and Z axes, and we did not use the residual surface because it is a step that significantly complicates the calculations. The obtained values of $\Delta\hat{X}$, $\Delta\hat{Y}$ and $\Delta\hat{Z}$ represent the translation parameters on all of the three axes, respectively. Hence, calculations in a network of highly precise leveling in the iterative procedure based on the latitudes φ_i and longitudes λ_i of the points P_i, and the differences ($t_i^{GOCO05c}$, $t_i^{SGG-UGM-2}$, $t_i^{XGM\,2019e}$) between the height anomaly ($\zeta_i^{GOCO05c}$, $\zeta_i^{SGG-UMG-2}$, $\zeta_i^{XGM2019e}$) and $\zeta_i^{GNSS/dh}$ at the same points, the translation parameters for all three are calculated, where j is the number of iterations. The values in the zero iteration (j = 0) are given in Table 5.

Table 5: GGM translation parameters in $j = 0$ iteration (unit: meter, n=1001).

GGM	$\Delta\hat{X}_0$	$\Delta\hat{Y}_0$	$\Delta\hat{Z}_0$
GOCO05c	1.30	1.54	-1.82
SGG-UGM-2	-1.64	1.04	1.20
XGM2019e	-1.64	1.58	1.00

Based on these values, it is possible to estimate the vector of differences $\hat{t}$, and according to equation (5), it is possible to obtain vector elements $\hat{t}_i$ representing a three-parameter transformation. Estimated differences $\hat{t}_i$ in all 1001 points in the zero iteration for all three GGM were statistically processed, and

for each was obtained: average value $\hat{t}^{GGM}_{average}$, minimum value $\hat{t}^{GGM}_{min}$, maximum value $\hat{t}^{GGM}_{max}$, range $\hat{t}^{GGM}_{range}$, and standard deviation σ^{GGM}_{i} (Table 6).

Table 6: Statistics of the estimated $\hat{t}^{GGM}$ (iteration $j = 0$) (unit: meter, n=1001).

$\hat{t}^{GGM}$	$\hat{t}_{\min}$	$\hat{t}_{\max}$	$\hat{t}_{average}$	$\hat{t}_{range}$	$\sigma_{\hat{t}(STDEV)}$
$\hat{t}^{GOCO05c}$	-0.11	0.08	0.00	0.19	0.04
$\hat{t}^{SGG-UGM-2}$	-0.05	0.04	0.00	0.09	0.02
$\hat{t}^{XGM\,2019e}$	-0.05	0.05	0.00	0.10	0.02

In the next step are obtained values of height anomalies after the transformation (Table 7):

$$\hat{\zeta}^{GGM}_{i} = \zeta^{GGM}_{i} - \hat{t}^{GGM}_{i}, \tag{10}$$

where $\hat{\zeta}^{GGM}_{i}$ are estimated GGM-derived height anomaly from the GOCO05c, SGG-UGM-2, and XGDM2019e models, ζ^{GGM}_{i} GGM-derived height anomaly from the GOCO05c, SGG-UGM-2, and XGDM2019e models, and $\hat{t}^{GGM}_{i}$ are values of estimated differences from equation (5) for all three GGM's.

Table 7: Statistics of the estimated $\hat{\zeta}^{GGM}$ (iteration $j = 0$) (unit: meter, n=1001).

$\hat{\zeta}^{GGM}$	$\hat{\zeta}_{\min}$	$\hat{\zeta}_{\max}$	$\hat{\zeta}_{average}$	$\hat{\zeta}_{range}$	$\sigma_{\hat{\zeta}(STDEV)}$
$\hat{\zeta}^{GOCO05c}$	42.29	46.15	44.59	3.86	0.86
$\hat{\zeta}^{SGG-UGM-2}$	42.23	46.28	44.52	4.05	0.85
$\hat{\zeta}^{XGM\,2019e}$	42.20	46.21	44.51	4.01	0.84

The values of GNSS/dh-derived height anomaly $\zeta^{GNSS/dh}_{i}$ is subtracted from the estimated value $\hat{\zeta}^{GGM}_{i}$, which gives differences (Table 8):

$$R^{GGM}_{i} = \hat{\zeta}^{GGM}_{i} - \zeta^{GNSS/dh}_{i}. \tag{11}$$

Table 8: Statistics of the diffrences R^{GGM}_{i} (iteration $j = 0$) (unit: meter, n=1001).

R^{GGM}	$R_{\min}$	$R_{\max}$	$R_{average}$	R_{range}	$\sigma_{R(STDEV)}$
$R^{GOCO05c}$	-0.32	0.18	-0.05	0.51	0.09
$R^{SGG-UGM-2}$	-0.49	0.12	-0.12	0.61	0.07
$R^{XGM\,2019e}$	-0.43	0.11	-0.13	0.54	0.08

At the end of each iteration, the GGM-derived estimated height anomaly from all three GGM's and the SQM2011-derived height anomaly are compared at 1001 points. In other words, we compared GGM values at interpolated height anomalies from SQM2011. The differences between these values are statistically processed, and the characteristic values are given in Table 9.

Table 9: Statistics of the differences $\Delta\hat{\zeta}$ (unit: meter, n=1001).

$\Delta\hat{\zeta} = \hat{\zeta}^{GGM} - \zeta^{SQM2011}$	$\Delta\hat{\zeta}_{\min}$	$\Delta\hat{\zeta}_{\max}$	$\hat{}_{average}$	$\Delta\hat{\zeta}_{range}$	$\sigma_{\Delta\hat{\zeta}(STDEV)}$
$\Delta\hat{\zeta} = \hat{\zeta}^{GOCO05c} - \zeta^{SQM2011}$	-0.29	0.16	-0.03	0.45	0.08
$\Delta\hat{\zeta} = \hat{\zeta}^{SGG-UGM-2} - \zeta^{SQM2011}$	-0.45	0.05	-0.10	0.50	0.06
$\Delta\hat{\zeta} = \hat{\zeta}^{XGM2019e} - \zeta^{SQM2011}$	-0.40	0.03	-0.11	0.43	0.07

The average value of the differences thus obtained should be equal to zero. However, this is not the case, which is why it is necessary to reduce the values of the vector R so that the average value weighs toward zero. Therefore, the values of the vectors of the estimated parameters $\hat{\mathbf{x}}_{3\times1}$, vector of free terms $\mathbf{f}_{n\times1,}$ and vector $\mathbf{n}_{n\times1}$ belong to the zero iteration. Each subsequent iteration involves a change of vector $\mathbf{f}_{n\times1}$:

$$\mathbf{f}^{GGM}_{n\times1\ (j)} = \begin{bmatrix} \hat{t}^{GGM}_{1,(j)} - t^{GGM}_{1} \\ \vdots \\ \hat{t}^{GGM}_{i,(j)} - t^{GGM}_{i} \\ \vdots \\ \hat{t}^{GGM}_{n,(j)} - t^{GGM}_{n} \end{bmatrix}_{n\times1}, \tag{12}$$

where are: $\hat{t}^{GGM}_{i,(j)}$ – estimated differences from (j) iteration, and t^{GGM}_{i} is the differences derived from equations (4). In the next iteration (first, j =1), the recalculation of previous results is continued to achieve the best possible adjustment of the surfaces obtained from the GGM's and GNSS/dh observations with the surface of the SQM2011. Therefore, after the iterative change, the vectors $\mathbf{f}_{n\times1}$, $\mathbf{n}_{n\times1}$ and $\hat{\mathbf{x}}_{3\times1}$ are recalculated, where the values of the vector $\hat{\mathbf{x}}_{3\times1}$ in the new iteration (j = 1) represent increments (Table 10) that are added to the estimated parameters from the previous iteration thus obtaining the final translation parameters (Table 10), i.e.:

$$\hat{\mathbf{x}}^{GGM}_{3\times1\ (j=1)} = \begin{bmatrix} d^{GGM}_{\Delta\hat{X}\ (j=1)} \\ d^{GGM}_{\Delta\hat{Y}\ (j=1)} \\ d^{GGM}_{\Delta\hat{Z}\ (j=1)} \end{bmatrix} \rightarrow \begin{cases} \Delta\hat{X}^{GGM}_{(j=1)} = \Delta\hat{X}^{GGM}_{(0)} + d^{GGM}_{\Delta\hat{X}\ (j=1)} \\ \Delta\hat{Y}^{GGM}_{(j=1)} = \Delta\hat{Y}^{GGM}_{(0)} + d^{GGM}_{\Delta\hat{Y}\ (j=1)} \\ \Delta\hat{Z}^{GGM}_{(j=1)} = \Delta\hat{Z}^{GGM}_{(0)} + d^{GGM}_{\Delta\hat{Z}\ (j=1)} \end{cases}. \tag{13}$$

The procedure is repeated in the same way as in the zero iteration, so there is no need to repeat the explanation. Only the numerical (Tables 11, 12, 13, and 14) and graphical (Figure 4) results of the first iteration are given below. The whole procedure is described additionally in the algorithm on Figure 2.

Table 10: Increments and translation parameters in $j = 1$ iteration (unit: meter, n=1001).

GGM	Increments			Translation parameters		
	$d_{\Delta\hat{X}_1}$	$d_{\Delta\hat{Y}_1}$	$d_{\Delta\hat{Z}_1}$	$\Delta\hat{X}_1$	$\Delta\hat{Y}_1$	$\Delta\hat{Z}_1$
GOCO05c	-0.03	-0.01	-0.03	1.27	1.53	-1.86
SGG-UGM-2	-0.08	-0.03	-0.08	-1.71	1.01	1.12
XGM2019e	-0.09	-0.03	-0.09	-1.73	1.55	0.91

Table 11: Statistics of estimated $\hat{t}^{GGM}$ (unit: meter, n=1001).

$\hat{t}^{GGM}$	$\hat{t}_{\min}$	$\hat{t}_{\max}$	$\hat{t}_{average}$	$\hat{t}_{range}$	$\sigma_{\hat{t}(STDEV)}$
$\hat{t}^{GOCO05c}$	-0.15	0.03	-0.05	0.19	0.04
$\hat{t}^{SGG-UGM-2}$	-0.16	-0.07	-0.12	0.09	0.02
$\hat{t}^{XGM2019e}$	-0.18	-0.08	-0.13	0.10	0.02

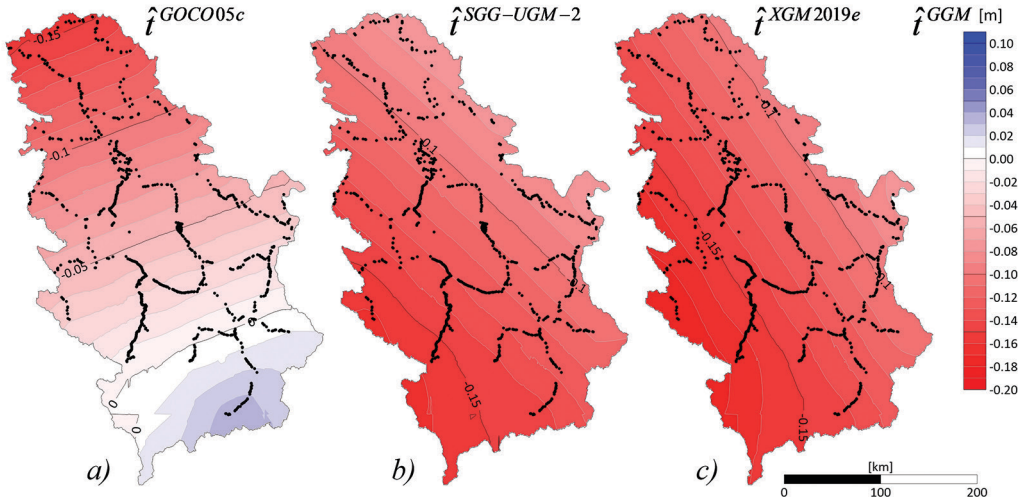

Figure 4: Contour plots of residuals $\hat{t}^{GGM}$ for a) GOCO05c, b) SGG-UGM-2 and c) XGM2019e (iteration j=1, n=1001).

Table 12: Statistics of $\hat{\zeta}^{GGM}$ (unit: meter, n=1001).

$\hat{\zeta}^{GGM}$	$\hat{\zeta}_{\min}$	$\hat{\zeta}_{\max}$	$\hat{\zeta}_{average}$	$\hat{\zeta}_{range}$	$\sigma_{\hat{\zeta}(STDEV)}$
$\hat{\zeta}^{GOCO05c}$	42.34	46.20	44.64	3.86	0.86
$\hat{\zeta}^{SGG-UGM-2}$	42.35	46.40	44.64	4.05	0.85
$\hat{\zeta}^{XGM2019e}$	42.33	46.34	44.64	4.01	0.84

Table 13: Statistics of R^{GGM} (unit: meter, *n*=1001).

R^{GGM}	$R_{\min}$	$R_{\max}$	$R_{average}$	R_{range}	$\sigma_{R(STDEV)}$
$R^{GOCO05c}$	-0.27	0.23	0.00	0.51	0.09
$R^{SGG-UGM-2}$	-0.37	0.24	0.00	0.61	0.07
$R^{XGM2019e}$	-0.30	0.24	0.00	0.54	0.08

Table 14: Characteristic values of $\Delta\hat{\zeta}$ (unit: meter, *n*=1001).

$\Delta\hat{\zeta} = \hat{\zeta}^{GGM} - \zeta^{SQM2011}$	$\Delta\hat{\zeta}_{\min}$	$\Delta\hat{\zeta}_{\max}$	$\Delta\hat{\zeta}_{average}$	$\Delta\hat{\zeta}_{range}$	$\sigma_{\Delta\hat{\zeta}(STDEV)}$
$\Delta\hat{\zeta} = \hat{\zeta}^{GOCO05c} - \zeta^{SQM2011}$	-0.24	0.21	0.02	0.45	0.08
$\Delta\hat{\zeta} = \hat{\zeta}^{SGG-UGM-2} - \zeta^{SQM2011}$	-0.33	0.17	0.02	0.50	0.06
$\Delta\hat{\zeta} = \hat{\zeta}^{XGM2019e} - \zeta^{SQM2011}$	-0.27	0.16	0.02	0.43	0.07

The iterative technique stops in the first iteration since the translation parameter increments are zero in the second iteration. Thus, all selected GGMs' final translation parameters were derived from the first iteration. All three GGM and GNSS/dh surfaces at 1001 high-precision leveling points matched SQM2011. We treated iterations defining translation parameters based on three selected GGMs and GNSS/dh measurements at high-precision leveling points as zero and first. The purpose of these iterations is to define the final values of translation parameters, which we used in the next part of the calculation to adjust the surface of GGM's with the surface of SQGM2011 on a grid of spatial resolution 1 km × 1 km throughout Serbia using three-parameter transformation.

5.2 Calculation procedure on the regular grid on the entire territory of the Republic of Serbia

After the procedure of defining translation parameters and obtaining their final values for all three chosen GGM's, the regular grid of mentioned resolution with 143207 points with known height anomaly ζ^{GGM} was defined for the entire territory of Serbia (Table 15) for which the estimated values of differences (Table 16) were calculated by three-parameter transformation based on the latitude and longitude of the grid points and the final translation parameters. The values of all three GGM's height anomalies on the same regular grid were modeled and corrected by the estimated differences. The obtained values are the estimated anomalous heights (Table 17). In this way, the surface derived from GGM's is adjusted based on SQM2011 for the entire territory of Serbia (Figure 5). Standard deviations, minimum, maximum, and mean values were calculated for the estimated GGM differences and corrected values of GGM height anomaly. Finally, corrected GGM height anomalies are compared to the SQM2011 height anomaly (Figure 6 and Table 18).

Table 15: Characteristic values ζ^{GGM} on a regular grid of 143207 points (unit: meter).

ζ^{GGM}	$\zeta_{\min}$	$\zeta_{\max}$	$\zeta_{average}$	ζ_{range}	$\sigma_{\zeta(STDEV)}$
$\zeta^{GOCO05c}$	40.97	46.35	44.57	5.39	0.93
$\zeta^{SGG-UGM-2}$	41.00	46.35	44.57	5.35	0.94
$\zeta^{XGM2019e}$	40.97	46.39	44.56	5.42	0.94

Table 16: Characteristic values of $\hat{t}^{GGM}$ (unit: meter, n=143207).

$\hat{t}^{GGM}$	$\hat{t}_{\min}$	$\hat{t}_{\max}$	$\hat{t}_{average}$	$\hat{t}_{range}$	$\sigma_{\hat{t}(STDEV)}$
$\hat{t}^{GOCO05c}$	-0.16	0.05	-0.05	0.21	0.05
$\hat{t}^{SGG-UGM-2}$	-0.19	-0.07	-0.12	0.12	0.03
$\hat{t}^{XGM2019e}$	-0.19	-0.07	-0.13	0.12	0.03

Table 17: Characteristic values of $\hat{\zeta}^{GGM}$ (unit: meter, n=143207).

$\hat{\zeta}^{GGM}$	$\hat{\zeta}_{\min}$	$\hat{\zeta}_{\max}$	$\hat{\zeta}_{average}$	$\hat{\zeta}_{range}$	$\sigma_{\hat{\zeta}(STDEV)}$
$\hat{\zeta}^{GOCO05c}$	41.01	46.38	44.62	5.37	0.89
$\hat{\zeta}^{SGG-UGM-2}$	41.07	46.51	44.69	5.44	0.96
$\hat{\zeta}^{XGM2019e}$	41.04	46.55	44.69	5.51	0.96

Table 18: Characteristic values of $\Delta\hat{\zeta}^{GGM}$ (unit: meter, n=143207).

$\Delta\hat{\zeta}^{GGM} = \hat{\zeta}^{GGM} - \zeta^{SQM2011}$	$\Delta\hat{\zeta}_{\min}$	$\Delta\hat{\zeta}_{\max}$	$\Delta\hat{\zeta}_{average}$	$\Delta\hat{\zeta}_{range}$	$\sigma_{\Delta\hat{\zeta}(STDEV)}$
$\Delta\hat{\zeta}^{GOCO05c} = \hat{\zeta}^{GOCO05c} - \zeta^{SQM2011}$	-0.85	0.53	-0.05	1.38	0.14
$\Delta\hat{\zeta}^{SGG-UGM-2} = \hat{\zeta}^{SGG-UGM-2} - \zeta^{SQM2011}$	-0.40	0.27	0.01	0.67	0.06
$\Delta\hat{\zeta}^{XGM2019e} = \hat{\zeta}^{XGM2019e} - \zeta^{SQM2011}$	-0.34	0.37	0.01	0.72	0.08

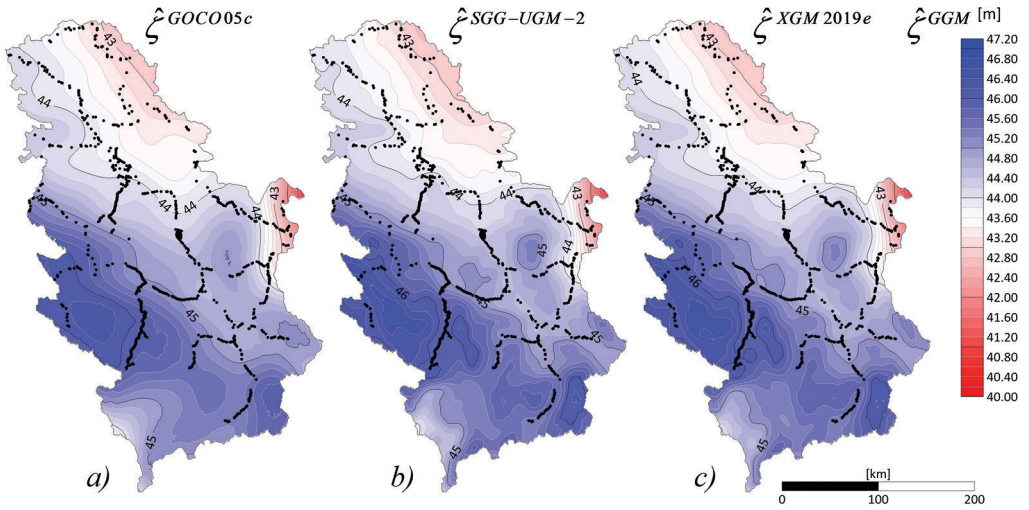

Figure 5: Modeled surfaces of $\hat{\zeta}^{GGM}$ for a) GOCO05c, b) SGG-UGM-2 and c) XGM2019e (n=143207).

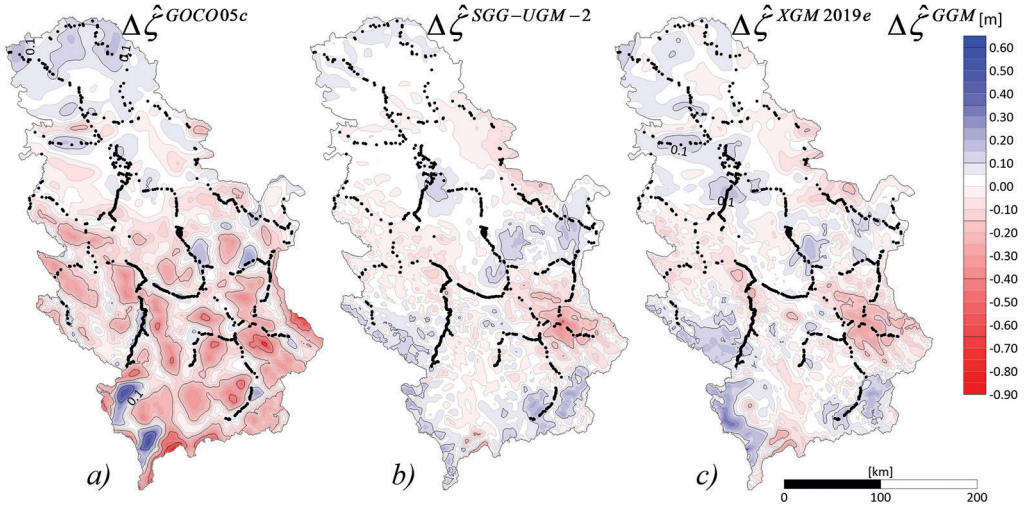

Figure 6: Modeled surfaces of $\Delta\hat{\zeta}^{GGM}$ for a) GOCO05c, b) SGG-UGM-2 and c) XGM2019e (n=143207).

6 CONCLUSION

This paper presents a study to evaluate and determine the quality of three GGM-derived reference surfaces using SQM2011 and GNSS/dh observations at 1001 points of the high-precision leveling network. The evaluation was performed using GGM (GOCO05c, SGG-UGM-2, and XGM2019e), SQM2011, and GNSS/dh-derived height anomaly, and calculated translation parameters based on a three-parameter transformation. In the evaluation process of local reference surface models derived from

GOCO05c, SGG-UGM-2, and XGM2019e for the territory of Serbia, the estimated anomalous heights are obtained in the following ranges. For the GOCO05c model, results go from a minimum of -0.85 m to the maximum value of 0.53 m, with an average of -0.05 m and a standard deviation of 0.14 m; for the SGG-UGM-2 model, the same statistical data are, -0.40 m, 0.27 m, 0.01 m and, 0.06 m; and for the XGM2019e model, -0.34 m, 0.37 m, 0.01 m and, 0.08 m. A detailed analysis found that the quality of these GGM-derived local reference surfaces is of sufficient accuracy for the needs of topographic survey, works in engineering projects, and GNSS height determination methods. Also, due to the constant improvement and development of global geopotential models, public availability of their data, increasing global territory coverage, and increasing degree and order, this method of defining local and regional reference surfaces can be strongly recommended. This recommendation is also supported by the fact that the necessary terrestrial data on local geodetic networks required for this method are frequently maintained with new terrestrial observations and geodetic surveys. This method is also supported by the latest research in Europe and the world, which evaluates the model of gravimetric quasigeoids using data obtained from GNSS/dh observations, and gives accuracy at the national level in the range of 1 cm to 2 cm and at the continental level in the range of 2 cm to 4 cm.

References

Adam, D. (2002, March 7). Gravity measurement: Amazing grace. Nature 416, 10-11. doi:https://doi.org/10.1038/416010a

Ågren, J., Đalović, S., & Škrnjug, J. (2012-02-26). Plan for the Future Determination of a National Geoid Model for Serbia. Republic Geodetic Authority (RGA) in Serbia, Belgrade.

Barthelmes, F. (2014). Global Models. Grafarend E (ed) Encyclopedia of Geodesy, 1-9. doi:10.1007/978-3-319-02370-0 43-1

Fecher, T. (2015). Globale kombinierte Schwerefeldmodellierung auf Basis voller Normalgleichungssysteme. München, Bayern, Deutschland: Technische Universität München (Technical University of Munich) - Lehrstuhl für Astronomische und Physikalische Geodäsie - TUM Engineering Faculty building Geo Environment (TUM Ingenieurfakultät Bau Geo Umwelt). Retrieved from http://mediatum.ub.tum.de/doc/1238858/555857.pdf

Fecher, T., Pail, R., & Gruber, T. (2015, February). Global gravity field modeling based on GOCE and complementary gravity data. International Journal of Applied Earth Observation and Geoinformation, Volume 35(Part A), 120-127. doi:https://doi.org/10.1016/j.jag.2013.10.005

Fecher, T., Pail, R., Gruber, T., & the_GOCO_Consortium. (2017, January 7). GOCO05c: A New Combined Gravity Field Model Based on Full Normal Equations and Regionally Varying Weighting. Surveys in Geophysics, Volume 38(issue 3), 571–590. doi:10.1007/s10712-016-9406-y

Heiskanen, W. A., & Moritz, H. (1967). Physical Geodesy (1st ed.). San Francisco and London: W. H. Freeman and Company.

Liang, W., Li, J., Xu, X., Zhang, S., & Zhao, Y. (2020, August). A High-Resolution Earth's Gravity Field Model SGG-UGM-2 from GOCE, GRACE, Satellite Altimetry, and EGM2008. Research Geodesy and Survey Engineering - Article, 6(8), 860-878. doi:https://doi.org/10.1016/j.eng.2020.05.008

Odalović, O. (2010). Fizička geodezija (1st ed.). Beograd, Srbija: Građevinski fakultet Univerziteta u Beogradu.

Odalović, O. R., Stanković, M. D., Grekulović, S. M., Joksimović, D. S., & Drakul, M. S. (2018a). Određivanje komponenti odstupanja vertikale primenom globalnog geopotencijalnog modela EGM2008 - Determination of deflection of the vertical components by using global geopotential model EGM2008. Tehnika, 73(3), 333-338. doi:10.5937/tehnika18033330

Odalović, O., Grekulović, S., & Vasiljević, I. (2018b). Globalni geopotencijalni modeli - Global Geopotential Models. Belgrade, Serbia: University of Belgrade - Faculty of Civil Engineering - Department of Geodesy and Geoinformatics.

Odalović, O., Joksimović, D., Petković, D., Stanković, M., & Grekulović, S. (2020). Evaluation and tailoring of global geopotential models in the determination of gravity field in Serbia. Proceedings of International Conference on Contemporary Theory and Practice in Construction XIV, 77-90. doi:10.7251/STP20140770

Odalović, O., Starcević, M., Grekulović, S., Burazer, M., & Aleksić, I. R. (2012). The establishment of a new gravity reference frame for Serbia. Survey Review, 44(327), 272-281. doi:10.1179/1752270611Y.0000000033

Pavlis, N. K., Holmes, S. A., Kenyon, S. C., & Factor, J. K. (2012, April). The development and evaluation of the Earth GravitationalModel 2008 (EGM2008). Journal of Geophysical Research: Solid Earth (AGU Journal), 117(B4). doi:https://doi.org/10.1029/2011JB008916

Rebhan, H., Aguirre, M., & Johannessen, J. A. (2000). The Gravity Field and Steady-State Ocean Circulation Explorer Mission – GOCE. Earth Explorer Mission, 6-11.

Reigber, C., Lühr, H., & Schwintzer, P. (Eds.). (2003). First CHAMP Mission Results for Gravity, Magnetic and Atmospheric Studies. Berlin, Heidelberg, Germany: Springer - Verlag GmbH. doi:10.1007/978-3-540-38366-6

Sjöberg, L. E. (1991). Refined least squares modification of Stokes' formula. Manuscripta geodaetica, 16(6), 367-375.

Sjöberg, L. E. (2003a, October). A computational scheme to model the geoid by the

modified Stokes formula without gravity reductions. Journal of Geodesy, 77, 423–432. doi:https://doi.org/10.1007/s00190-003-0338-1

Sjöberg, L. E. (2003b, May). A solution to the downward continuation effect on the geoid determined by Stokes' formula. Journal of Geodesy, 77, 94–100. doi:https://doi.org/10.1007/s00190-002-0306-1

Sjöberg, L. E., & Nahavandchi, H. (2000, January). The atmospheric geoid e¡ects in Stokes' formula. Geophysical Journal International, 140(1), 95-100. doi:https://doi.org/10.1046/j.1365-246x.2000.00995.x

Veljković, Z., Lazić, S., & Jivall, L. (25 - 28 May 2011). Results of the EUREF Serbia 2010 Campaign. Republic Geodetic Authorty of Republic of Serbia, bul. Vojvode Mišića 39, The Sector for Basic Geodetic Works. Chisinau, Moldova: Symposium of the IAG Subcommission for Europe (EUREF). Retrieved from http://www.euref.eu/symposia/2011Chisinau/06-01-p-Veljkovic.pdf

Vušović, N., Svrkota, I., & Vaduvesković, Z. (2013). Prostorni referentni sistem Republike Srbije - Spatial Reference System of Serbia. Rudarski radovi - Mining Engineering, 1. doi:10.5937/rudrad1301049V

Zingerle, P., Pail, R., Gruber, T., & Oikonomidou, X. (2020, July 20). The combined global gravity field model XGM2019e. Journal of Geodesy, 94(66). doi:https://doi.org/10.1007/s00190-020-01398-0

Stanković M., Odalović O., Marković M. (2022). Validation and comparison of several Global Geopotential Models with an official quasigeoid solution of Serbia. Geodetski vestnik, 66 (3), 432-448.
DOI: https://doi.org/10.15292/geodetski-vestnik.2022.03.432-448

Marko Stanković, M.Sc. Geodesy
Department of Geodesy and Geoinformatics,
Faculty of Civil Engineering, University of Belgrade
Bul. kralja Aleksandra 73, 11120, Belgrade, Serbia
e-mail: stankovic.d.marko@gmail.com

Miloš Marković, M.Sc. Geodesy.
Department of Geodesy and Geoinformatics,
Faculty of Civil Engineering, University of Belgrade
Bul. kralja Aleksandra 73, 11120, Belgrade, Serbia
e-mail: milmarkovic85@gmail.com

Assoc. Prof. Oleg Odalović, Ph. D. Sci. Geod. Eng.
Department of Geodesy and Geoinformatics,
Faculty of Civil Engineering, University of Belgrade
Bul. kralja Aleksandra 73, 11120, Belgrade, Serbia
e-mail: odalovic@grf.bg.ac.rs